The Journal of Adhesion, 78: 723–739, 2002

0021-8464/02 $12.00 +.00
DOI: 10.1080/00218460290010458

STRAIN RATE DEPENDENCE OF FRACTURE IN A RUBBER-TOUGHENED EPOXY SYSTEM

D. Raghavan and J. He
Polymer Science Division, Department of Chemistry, Howard University, Washington, DC, USA

D. Hunston
Building Materials Division, National Institute of Standards and Technology, Gaithersburg, Maryland, USA

D. Hoffman
The Dow Chemical Company, Midland, Michigan, USA

The toughening mechanisms in rubber-modified epoxies appear to be viscoelastic in nature since their fracture behavior is dependent on loading rate. This behavior has been studied in detail and modeled for only one system, a model toughened epoxy often used in research work. The present study examines the loading rate effect for a new material based on acrylic rubber by measuring the fracture energy in constant cross-head speed tests conducted over a wide range of speeds. As expected, decreasing the loading rate produced an increase in toughness. Just as in the previous studies, the fracture energies could be modeled with a power law relationship when the loading rate was characterized by the time to failure. Moreover, the parameters involved in the model are quite consistent with the earlier results. For most rates, the behavior was approximately linear elastic with little or no r-curve behavior. Below a critical rate, however, there was a transition to ductile failure with a large r-curve and very high fracture energies. The transition is very

Received 13 April 2001; in final form 19 April 2002.

The authors thank the Polymer Division of NIST, AFOSR, and the Department of Chemistry at Howard University for providing financial support to Mr. J. He. The authors would also like to thank X. Gu for the atomic force microscopy studies of morphology. Certain commercial materials and equipment are identified in this paper in order to specify adequately the experimental procedure. In no case does such identification imply recommendation or endorsement by the National Institute of Standards and Technology, nor does it imply necessarily that the items are the best available for the purpose.

Address correspondence to Prof. D. Raghavan, Polymer Science Division, Deparment of Chemistry, Howard University, Washington, DC 20059, USA. E-mail: draghavan@howard.edu

sudden which may help explain why some previous studies have observed this effect while others have not.

Keywords: Acrylic rubber, Epoxy, Fracture, Rate effects, r-curve, Toughening, Viscoelastic

INTRODUCTION

Thermoset polymers are widely used in structural adhesives and composites because such polymers have many desirable properties such as high modulus and low creep over a wide range of temperatures. Unfortunately, an important limitation is that most thermosets are very brittle. In response to this weakness, industry has developed the technology that permits some thermosets to be toughened by the addition of a second phase which forms small particles, typically in the micrometer range, that are dispersed in and bonded to the thermoset matrix. By using a phase-separated morphology, the toughness can be increased dramatically with a minimal sacrifice in other properties [1–9]. Over the past 35 years, industry has formulated a wide variety of toughened systems, mostly based on epoxy. Many of these systems use carboxyl-terminated butadiene acrylo-nitrile (CTBN) in the second phase.

Scientific studies of these materials have been conducted since the late 1960s and have examined many aspects of the toughening behavior [1–9]. One important conclusion of this research is that the toughening mechanisms are generally viscoelastic in nature and so the fracture energy depends on temperature and loading rate [7–13]. Although this behavior is well known, it has been studied and/or modeled for only a small number of material systems. As a result, there is a question as to whether other toughened thermosets behave in a similar manner or exhibit significant differences. Modeling such behavior is critical, so that different systems can be compared and performance over a wide range of conditions can be predicted. The absence of this predictive capability now requires designers to include large safety factors and use conservative measures of toughness. The result is added cost and loss of design flexibility for the users of adhesive joints. The purpose of this paper is to extend the studies of viscoelastic fracture to a new type of toughened epoxy and compare the results with previous work. In addition, the fracture behavior was examined to see whether resistance curve (r-curve) behavior is present. In a r-curve, the fracture energy increases as the crack grows until the growth becomes unstable or a steady state growth at an

approximately constant fracture energy is achieved. Historically, studies of toughened epoxies have found little or no evidence of r-curve behavior, but several recent papers have reported very significant r-curves [14−17]. What makes this result particularly interesting is that the material systems and test methods in the recent work are quite similar to those used in the previous studies.

BACKGROUND

The most commonly used model material system for toughening experiments is a di-functional epoxy, di-glycidyl ether of bisphenol A (DGEBA) with CTBN as the toughener and cured with an appropriate curing agent [3−6]. CTBN is a polymer, but the molecular mass is low enough that it is compatible with the DGEBA. When the DGEBA-CTBN mixture is cured, the reactions involve polymerization of the epoxy and copolymerization of the epoxy and CTBN. As the molecular masses increase, the molecules containing CTBN become incompatible with the epoxy and phase separate to form discrete elastomer particles. Sometimes the phase separation is very complete, while in other cases some elastomer units remain in the epoxy matrix. This and other morphological features such as the particle sizes and the size distribution depend on the chemistry and cure history. By varying concentrations, constituents, and cure history, a wide variety of morphologies can be generated. Each morphology has a different fracture behavior but, in all cases, the resistance to fracture depends on loading rate and temperature. This commonality in behavior suggests that it might be possible to formulate a general model to describe the fracture of such systems.

Despite the widespread knowledge that the fracture behavior of such systems depends on loading history [7−13], there have been relatively few detailed studies of loading rate and temperature effects. The most extensive study, conducted by Hunston et al. [11−12], examined four different materials based on DGEBA and CTBN cured with piperidine. Although these materials have glass transition temperatures that are low relative to most commercial-structural adhesives, the fracture behavior closely simulates that seen in commercial materials. To generate three of the four model systems, the concentration of CTBN was varied. In the fourth system, a small amount of bisphenol-A was added to the mixture before curing. The addition of bisphenol-A produced a major change in morphology so that the cured material has a bimodal distribution of particle sizes with both micrometer and submicrometer particles. The authors determined the fracture energies for these systems at different loading rates and

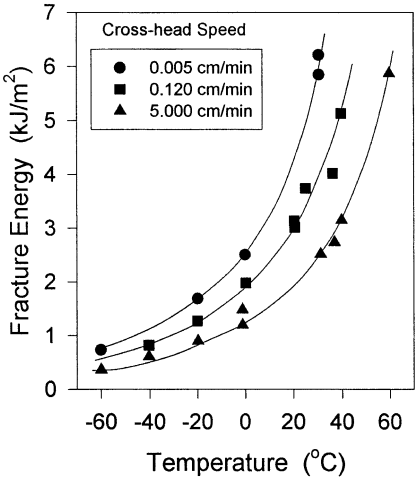

FIGURE 1 Fracture energy as a function of temperature at 3 different cross-head speeds for CTBN-epoxy system [12]. Lines are arbitrary, smooth curves drawn through the points to help visualize the data. Relative uncertainty for the fracture energies is 10%.

temperatures, and some typical results are shown in Figure 1, which gives the mode-I fracture energy (G_{IC}) for temperatures between $-60°C$ to $+60°C$ at three cross-head speeds. The results show that increasing the temperature produces a similar effect to decreasing the loading rate. To model these data as a viscoelastic process, the authors chose to characterize the loading rate by determining the time to failure t_f, i.e., total elapsed time between the initial application of load and the onset of rapid or stable crack growth.

Why did the authors use t_f as the independent variable? The important parameter in such experiments is the loading rate of the material in the crack-tip region. Unfortunately, local loading rate is not only difficult to measure but also varies with position so an alternative is needed. This alternative should be both measurable and directly related to the loading rate in the crack-tip region. The most commonly used parameter with a moving crack is the crack propagation velocity. This parameter provides a direct indication of how rapidly the material ahead of the crack is loaded as the crack approaches. For the experiments in Figure 1, however, crack velocity is not appropriate since the fracture values correspond to the transition from no crack growth or very slow crack growth to rapid propagation. If the crack does not move prior to the onset of rapid crack growth, then t_f furnishes a good measure of loading rate for the

material near the crack tip. Moreover, there is some justification for thinking that it might be independent of crack length since it always measures the time required for the crack-tip region to load up to the failure point. If the crack moves more than a very short distance prior to the failure point, then the basis for using t_f is violated. Thus, this approach is valid only for a particular class of results.

By using t_f and the principle of time–temperature superposition, the authors [11–12] modeled the G_{IC} data with a simple empirical equation containing a power law expression in t_f, and an Arrhenius-like term for temperature:

$$G_{IC} = G_{ICB} + C\, e^{-\frac{\Delta E}{RT}} t_f^m. \tag{1}$$

There are 4 adjustable constants in the equation: G_{ICB}, which measures the limiting toughness at low temperature and high loading rates; C, which characterizes the magnitude of the toughening effect; ΔE, which indicates the temperature sensitivity; and m, which describes how rapidly the fracture energy varies with loading rate. R is the gas constant, and T is the absolute temperature.

If the four adjustable constants in Equation (1) are determined, the fracture behavior can be predicted over a wide range of conditions. Of course, extrapolating outside the range where testing is done can be dangerous. For example, Equation (1) indicates that the fracture energy will continue to increase as the temperature is raised, but this prediction will eventually fail since the toughness will go down once the temperature gets above the glass transition temperature. Another important feature of Equation (1) is that it facilitates comparison of different materials. For the four systems mentioned above [12], the values of ΔE were found to be identical, and this was attributed to the fact that this parameter depended on the nature of the matrix, which was nearly identical for all four materials. The value of m was found to vary only when the morphology was significantly altered; i.e., the sample, which contained a bimodal distribution of particle sizes, had a different value of m from the other three systems. The value of C depended on both the rubber concentration and morphology. Unfortunately, the generality of such observations is limited by the small amount of data available. The work here seeks to address this issue by examining the viscoelastic fracture of a new type of toughened epoxy.

This new materials system uses preformed rubber particles. A number of authors and companies have investigated this technology because preforming the rubber particles before cure locks in the morphology so it is no longer an uncontrolled variable. The particular

system used here is based on the material developed by the Dow Chemical Co. [18–20]. The starting material is generated by forming a suspension of acrylic rubber particles in a liquid epoxy. In earlier papers [21–27], the effect of changing the particle concentration at a fixed morphology was examined by diluting the acrylic rubber suspension with different amounts of liquid epoxy before curing the system. The results show that the fracture energy of the acrylic system goes through a maximum with increasing concentration of rubber particles. This behavior is similar to what had been observed for CTBN materials, except that the maximum was about twice as high and occurred at a lower rubber concentration for the acrylic material. The limitation in this work is that the fracture behavior was measured only at a single cross-head speed. The data reported here extends the research by measuring the fracture behavior as a function of loading rate.

EXPERIMENTAL PROCEDURE

Materials and Methods

The starting material was generated by the procedure developed at Dow Chemical Co. and published in the literature [18–20]. The resulting suspension contained acrylic rubber particles (copolymer of 2-ethylhexyl acrylate and glycidyl methacrylate) dispersed in a liquid epoxy resin (Dow Tactix 123 LER, a diglycidyl ether of bisphenol A {DGEBA}-type resin). Samples were prepared by diluting this suspension with the appropriate amount of liquid epoxy and hand stirring for 5 to 10 min. The mixture was degassed under vacuum in a Fisher Scientific Isotemp Vacuum Oven Model 281A at 50 to 60°C until foaming stopped (about 3 h). After cooling to room temperature, 5 g of piperidine were added for every 100 g of the epoxy. The resulting mixture was poured into a preheated mold and cured in an oven at 120°C for 16 h. The heater was then turned off, and the sample was allowed to cool slowly in the closed oven so that all samples had the same thermal history. Test specimens were machined from the molded plates. Samples were prepared with 3 different rubber concentrations: 5 g, 10 g, or 20 g of preformed rubber particles for every 100 g of epoxy. The concentrations are designated here by mass ratio (mr) of rubber to epoxy, so values are 0.05 mr, 0.10 mr, and 0.20 mr.

Characterization of Rubber-Dispersed Epoxy

In the previous study with the acrylic rubber-epoxy samples [25], TEM (Transmission Electron Microscopy) was used to examine morphology. Although this was very informative, the sample preparation is difficult

and time consuming, so there is a need for an alternate approach that is fast and simple. One possibility is atomic force microscopy (AFM), so the work here examined the samples using tapping mode atomic force microscopy (TMAFM). These tests were performed with a Dimension 3100 (Digital Instruments, Santa Barbara, CA) scanning probe microscope with topographic (height) and phase images recorded simultaneously at ambient conditions. Commercial silicon cantilever probes, each with a nominal tip radius of 5 nm to 10 nm and spring constant in the range of 20 N/m to 100 N/m (values provided by manufacturer) were oscillated at the mode I fundamental resonance frequency. At certain levels of tapping force, images were recorded. Changes in the phase of the oscillating probe were used to produce a contrast between the epoxy and the acrylic rubber regions. All images were recorded using a free-oscillation amplitude of 60 nm (standard uncertainty of ± 2 nm).

Strain Rate Studies

Details of sample preparation, characterization, and testing are outlined in the earlier paper [23–27] and will only be briefly mentioned in this section. The fracture tests were performed with compact test specimens loaded at a constant cross-head speed until failure. The cross-head speeds ranged from 2 cm/min to 0.001 cm/min which is the range that can conveniently be done on a standard tensile machine. For selected specimens, a grid was marked on the side of the sample, and the crack growth was monitored throughout the test. For the very low speed experiments, where considerable slow crack growth was observed, a video microscope was used to follow crack growth. The standard uncertainty in the crack length measurement was ± 0.5 mm without the microscope and ± 0.1 mm with the microscope. The mode-I fracture energies, G_{IC}, were calculated using the standard equation given in ASTM E-399 [23–27]. In addition, each fracture experiment was also characterized by measuring the time to failure, i.e., the total elapsed time between the initial application of load and the onset of rapid or steady-state crack growth (t_f). The modulus values required for the calculations were determined with 3-point bend tests (ASTM D-790) conducted as a function of time. The times to failure in the fracture tests were used to select the appropriate values of moduli for the tests [9, 11, 27]. For each composition, 5 specimens were used to determine the average modulus. In the fracture tests, the sample thickness for the compact tension specimens was 1.27 cm. At least 5 fracture tests were performed at each set of conditions and compositions.

RESULTS AND DISCUSSION

Characterization of Rubber-Dispersed Epoxy

Figure 2 shows AFM topographic (left) and phase (right) images for a sample with 20 mr acrylic rubber. As shown in the figure, each image is for an area on the surface that is 10.0 μm by 10.0 μm. The height scale is 100 nm and the phase scale is 40°. The images show some distinct features, most notably, the circular domains. The largest domains are just over 5 μm in diameter, and the dark color in the topographic image indicates that these regions are depressed with respect to the surrounding area. These same domains are seen in the phase image as light regions.

The shape of these domains suggests that they are the acrylic particles, and there are three pieces of evidence that support this hypothesis. First, the size is a good match for the particle diameter obtained previously in the TEM studies [25]. Second, it is known that the rubber domains in toughened systems often appear as depressions in the surface of cross-sectioned samples. This is attributed to the fact that the rubber has a higher thermal expansion coefficient than that of the surrounding glassy polymer. When the sample is cooled following cure, the rubber is prevented from contracting as much as it would like to by the surrounding glassy resin. When the sample is cut, however, the constraint is released along the free surface and the rubber contracts forming a depression. The third piece of evidence is a

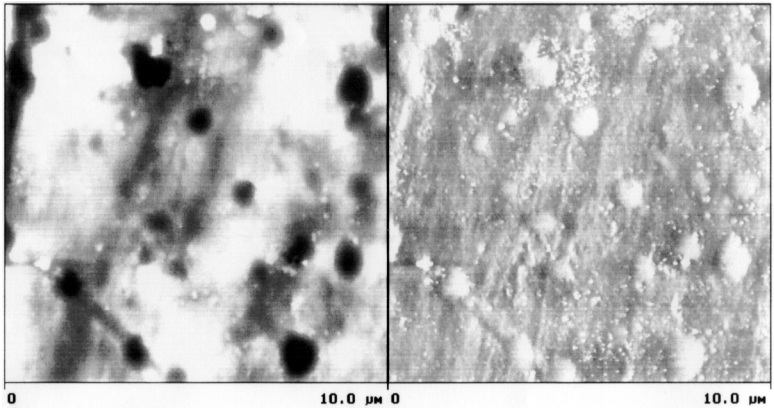

FIGURE 2 Tapping mode AFM: height image (left) and phase image (right) for the 0.20 mr acrylic rubber modified epoxy. Contrast variations are 100 nm from light to dark for the height image and 40° from light to dark for the phase image.

measurement of the area fraction on the surface occupied by the circular domains. This is one of several standard AFM methods used to identify the domain and matrix components in a phase-segregated system [28–30]. Image analysis was used to examine the phase image in several 10 μm × 10 μm images. Only a small area on the sample was analyzed, but the result—approximately 20% of the scan area occupied by the circular domains—is in good agreement with the expected value based on the concentration of acrylic rubber. To test this result, a similar analysis was conducted on a sample made with 0.10 mr acrylic particles in epoxy. The area fraction occupied by the circular domains is roughly 10% in this sample. This indicates that AFM is a useful method to study morphology in these materials.

Fracture Studies

Like any toughened thermoset, the fracture of acrylic-modified epoxy exhibits three types of failure, as illustrated in Figure 3. At higher loading rates, brittle-unstable crack growth is observed (curve A). The loading curve shows linear elastic behavior up to a critical load where failure occurs by the onset of rapid crack growth. The fracture surface is characterized by a small region of stress-whitened material just ahead of the initiation point. This indicates significant deformation and plastic flow in the resin. Beyond this zone, the surface is smooth and glassy corresponding to rapid crack growth. Microscopic examination of the glassy surface indicates little resin deformation. The second type of failure occurs at the lowest loading rates and intermediate rubber concentration where the toughness is highest. This involves stable crack growth (curve C) and is characterized by linear elastic loading up to the point where the crack begins to advance slowly. The loading curve may continue to rise for a short time but

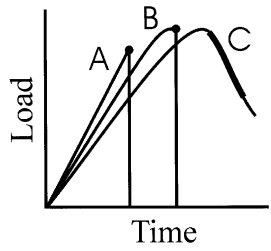

FIGURE 3 Three types of fracture behavior exhibited by toughened epoxy: unstable (A), stable-unstable (B), and stable (C). Enlarged dots and thick line indicate values used to calculate fracture energies.

diverges from linear behavior as the crack slowly accelerates. Soon, the load begins to fall and the crack growth reaches a steady state propagation rate driven by the motion of the cross-head. This occurs at a roughly constant value of G_{IC}. If the sample is unloaded, the load-displacement curve returns to the origin. The entire fracture surface is stress whitened, indicating deformation of the resin throughout the slow crack growth region. The third type of crack growth involves a combination of slow and unstable propagation (curve B). In this process, the crack begins to move slowly, but at some point the growth becomes unstable and the crack propagates rapidly. The fracture surface is stress whitened in the region of slow crack growth and for a short distance ahead of the initiation point for rapid crack propagation.

For the purpose of discussion, the failure process will be divided into two parts: the failure event itself and the initiation process that precedes it. The failure event and corresponding fracture energy, G_{IC}, will be defined here as the onset of rapid crack growth (solid point) in Figure 3, curves A and B, or the steady-state crack growth (wide line) in Figure 3, curve C. The effect of strain rate on these fracture energies will be covered first, and then the initiation process will be considered.

Strain Rate Effects on Fracture Energy

Figure 4 shows values for fracture energies defined as described above and measured using 3 different rubber concentrations and 4 cross-head speeds. The results are plotted against time to failure, t_f. For the open symbols (type A failure) t_f provides a good measure of loading rate in the crack tip region. With the filled symbols (type B failure) it is important to ask how far the crack grows before becoming unstable. For the result reported here this distance is very short, so t_f is a reasonable measure of loading rate. The filled symbols containing a plus sign correspond to stable crack growth. In this case, t_f is generally not an appropriate measure of loading rate.

The trends exhibited in Figure 4 are identical to those seen with the CTBN-epoxy. Lower loading rates produce higher fracture energies, while increasing rubber concentrations produce an increase in fracture energy followed by a reduction in G_{IC}. The rate effect can be understood by noting that the toughening is attributed to viscoelastic deformation processes that occur in a zone ahead of the crack tip [3, 7–9, 11]. There is a good correlation between the size of this deformation zone and the fracture energy. Since one manifestation of these deformations is stress whitening, it is not surprising that the fracture energy generally correlates with the size of the

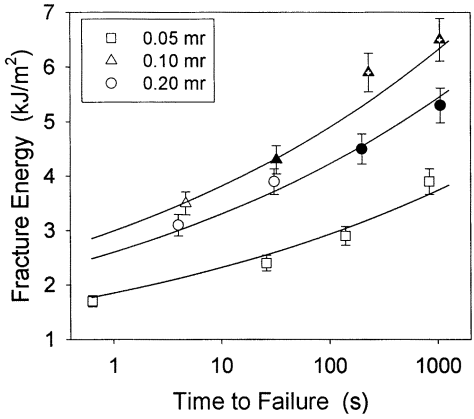

FIGURE 4 Fracture energies for acrylic-epoxy system measured at 3 concentrations and 4 different cross-head speeds. The cross-head speeds are characterized by recording the time to failure in each test. Open symbols are type A failure, the filled symbols are type B failure, and filled symbols with + sign are type C failure. The error bars indicate the standard uncertainty in the fracture data. The lines are best-fit curves with Equation (2).

stress-whitened region ahead of the crack tip. The amount of deformation (and zone size) will grow when the molecular mobility is increased by raising the temperature or the time available for deformation is increased by lowering the loading rate.

Equation (1) can be used to make a more quantitative comparison with the CTBN-epoxy results. Since temperature was not studied here, the temperature term and the coefficient C are grouped together as a new adjustable constant, C'. This leaves 3 adjustable parameters that may or may not be dependent on rubber concentration. Consequently, a simple curve fit is not very informative since there are at most 4 data points at each concentration. A more interesting comparison can be made by using the previous results to reduce the number of adjustable constants. The rationale for this is that although the composition of the particles is quite different in the acrylic rubber system, the matrix itself is very similar to that in the CTBN system. Both systems utilize a DGEBA-type epoxy cured with the same concentration of piperidine for 16 h and 120°C. With CTBN, the rate parameter, m, was independent of rubber concentration unless there were major changes in morphology such as going to a bimodal distribution of particle sizes. Consequently, the value of m that was determined previously (0.118) might be applicable here. The CTBN work also found that the limiting toughness at low temperatures and

TABLE 1 Best Fit Parameters for Equation (2)[a]

Rubber concentration	Toughening coefficient, C'	
Mass ratio	Acrylic system	CTBN system
0.05	1.50 ± 0.06	0.65
0.10	2.64 ± 0.07	1.05
0.20	2.25 ± 0.04	1.55

[a] Range on acrylic system indicates standard uncertainty; uncertainty not available from literature for CTBN System.

high rates, G_{ICB}, was a function of rubber concentration. On the other hand, the values were quite low relative to the toughness at room temperatures, so within the range of values that are reasonable the specific choice for G_{ICB} has little effect on the fit of the data. Consequently, the average value obtained in the previous study (0.35 kJ/m^2) will be used here for all concentrations. This leaves only one adjustable parameter, C', for each concentration:

$$G_{IC} = 0.35 + C' t_f^{0.118}. \tag{2}$$

Figure 4 shows best-fit curves of the points for types A and B failure using Equation (2), and the resulting values of C' are given in Table 1. The curves describe these data quite well. Surprisingly, even though the type C failure points are not included in the analysis, they fall relatively close to the curve. A possible explanation is that stable crack growth is established very quickly so there is relatively little crack growth prior to that. In this case, t_f may provide some indication of the loading rate in the crack tip region at the onset of steady growth. Nevertheless, including these points in the analysis would be open to question.

For comparison, Table 1 also lists the values that would be calculated for the CTBN-epoxy system measured under the same conditions. Comparing the parameters gives the same conclusion reached in the previous research; that is, the acrylic system appears to be tougher than the CTBN system for the same rubber concentration. At present, there is no explanation for what may be a very interesting result.

Fracture Initiation Behavior and the Effect of Strain Rate

The initiation behavior for fracture can be characterized by monitoring the crack growth as a function of the applied load. The first detectable crack growth generally corresponds to the lowest value of

fracture energy. This point is often difficult to determine and can be somewhat arbitrary since it may depend on the magnification used to monitor the crack tip. Moreover, it is difficult to separate what is true crack growth from what is blunting of the crack tip. Once the crack begins to move, the fracture energy usually increases and reaches a maximum at the point where the growth becomes unstable or where steady-state stable growth is achieved. The plot of crack growth versus fracture energy is called a resistance curve and can be used to describe the initiation process.

In many cases, there is little detectable crack growth in the initiation process, or the minimum and maximum fracture energies are very similar so that a single value of fracture energy can be used to characterize the failure. This is the case in much of the previous work on toughening. A recent series of papers [14–17], however, reported large r-curves with significant differences between the upper and lower limits and very high upper G_{IC} values. The materials and test conditions that were used were similar to those employed in the earlier studies where such behavior was not observed. This observation prompted the current study to examine the resistance behavior of the acrylic-epoxy system.

Figure 5 shows a plot of G_{IC} versus crack length at different loading rates for the acrylic material with a rubber concentration of 0.20 mr. Each curve represents data for a single sample selected because it was typical of the behavior at that rubber concentration. The initial studies examined rates between 0.01 cm/min and 2.00 cm/min. As seen in Figure 5, the results show relatively little r-curve behavior. Only at the slowest rate (0.01 cm/min) is there much difference between the initial value of G_{IC} and the maximum G_{IC}. Even in this case, the difference is small if the first point is not considered, and the initial point is often suspect because it is difficult to determine. What is clear from these results, however, is that the data show a trend toward more r-curve–like behavior as the cross-head speed is reduced. Based on this, a number of tests were conducted at even lower cross-head speeds using a video-microscope system to detect and quantify the crack growth more accurately. The curve in Figure 5 for a rate of 0.005 cm/min is an example. Under these conditions, a large r-curve is observed and very high fracture energies are achieved. This is very similar to the behavior recently reported in the literature [14–17].

There is some controversy about the validity of fracture energies as large as those found at this very slow rate. The thickness of the samples tested here (1.27 cm) is not adequate to give plane strain results using the ASTM criteria and the unloading curve does not return to the origin, indicating plastic deformation. Thouless et al. [17]

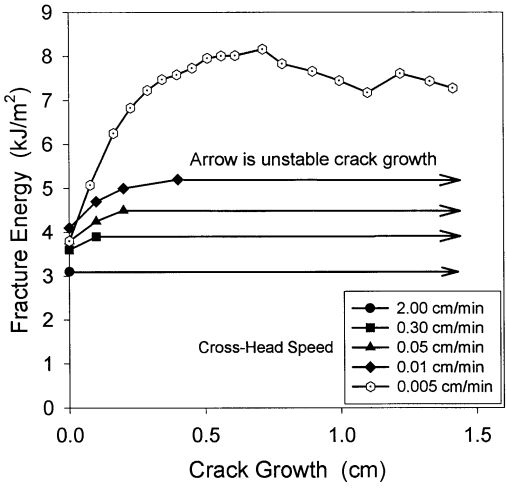

FIGURE 5 Resistance curve behavior for 0.20 mr samples of acrylic-epoxy system measured at 5 different cross-head speeds. The relative uncertainty in the fracture energies is 6%.

have conducted experiments that suggest these conditions may be too restrictive and have provided a possible explanation for the unloading curve not returning to the origin. It is not the purpose of this paper to address this controversy but simply to show that the type of r-curve reported in the literature can be obtained when these materials are tested under the right conditions. It is also interesting to note that the transition between the more brittle and ductile behavior is quite sudden. Changing the loading rate by a factor of 200 from 2.00 cm/min to 0.01 cm/min produces a modest change in behavior, while further lowering the rate by a factor of 2 causes the behavior to change dramatically. This may be one factor contributing to the fact that some authors see r-curve behavior while other researchers do not.

The initiation behavior can be rationalized using a very simple idea. It assumes that the toughness is related to the size of the deformation zone ahead of the crack tip, $\delta - \Delta a$, where Δa is the change in crack length produced by slow crack growth during loading and δ is total length of the deformation zone from where it starts at the end of the precrack ($\Delta a = 0$). The failure behavior can then be viewed as a competition between the growth of the deformation zone and the advance of the crack. When the sample is loaded, a critical value is reached where the deformation zone begins to grow. Subsequent loading eventually produces a condition where the crack begins to advance. As long as the deformation zone is growing more rapidly than the crack,

$d\delta/dt > d\Delta a/dt$, the toughness will increase with increasing crack length. If the loading rate is high enough, the crack growth rate will eventually exceed $d\delta/dt$. This will produce unstable crack propagation because the fracture resistance does go down as Δa increases. At high loading rates, the growth of the deformation is hindered so the toughness is lower, and there is little or no slow crack growth before propagation becomes unstable. As the loading rate is lowered, there is more deformation zone growth so the toughness is greater, and there is more slow crack growth prior to ultimate failure. If the loading rate is sufficiently low, the acceleration of the crack growth during initiation is slow enough that a stable region can be achieved where $d\delta/dt = d\Delta a/dt$. This results in stable crack growth at constant fracture energy. While this simple idea provides a rationale for the data, it is neither quantitative nor predictive. There is a real need for additional study to improve our understanding and ability to model the factors that control this behavior and the criteria that predict the transitions.

CONCLUSIONS

The following conclusions can be drawn from the current work:

1. The fracture behavior of acrylic-modified epoxy is quite similar to that for CTBN-modified epoxies. The fracture energy depends on loading rate and seems to be viscoelastic in that slower loading times permit more crack-tip deformation, which increases toughness.
2. The loading rate dependence of the fracture energies for the acrylic system can be fit with a power law relationship using time to failure as a measure of the rate parameter. The fit constants are consistent with those for CTBN-epoxy.
3. Lowering the loading rate produces a transition from unstable crack growth to mixed stable and unstable growth and eventually to stable growth with increasing fracture toughness. If the loading rate is decreased enough, there is a transition to a ductile type failure with a large r-curve. This transition occurs over a very small range of loading rates, which may help explain why some workers have seen the effect while others have not.
4. Tapping mode AFM was used to examine the morphology and study the composition of acrylate-modified epoxies. Compositional analysis was used to identify acrylate as the domain material associated with the lower lying regions in the height image.

REFERENCES

[1] Sultan, J. N., Laible, R. C. and McGarry, F. J., *J. Appl. Polym. Sci.* **6**, 127 (1971).
[2] Sultan, J. N. and McGarry, F. J., *Polym. Eng. Sci.* **13**, 29–34 (1973).
[3] Bascom, W. D., Collington, R. L., Jones, R. L. and Peyser, P. J., *J. Appl. Polym. Sci.* **19**, 2545–2562 (1975).
[4] Riew, C. K. and Gillham, C. K., in *Rubber-Modified Thermoset Resins*, Advances in Chemistry Series, No. 208 (American Chemical Society, Washington, DC, 1984).
[5] Riew, C. K., in *Rubber-Toughened Plastics*, Advances in Chemistry Series, No. 222 225–241 (American Chemical Society, Washington, DC, 1989).
[6] Riew, C. K. and Kinloch, A. J., in *Toughened Plastics I: Science and Engineering*, Advances in Chemistry Series, No. 233 (American Chemical Society, Washington, DC, 1984), and *Toughened Plastics II: Science and Engineering*, Advances in Chemistry Series, No. 252 (American Chemical Society, Washington, DC, 33–44 1996).
[7] Kinloch, A. J., Shaw, S. J., Tod, D. A. and Hunston, D. L., *Polymer* **24**, 1341–1354 (1983).
[8] Kinloch, A. J., Shaw, S. J. and Hunston, D. L., *Polymer* **24**, 1355–1363 (1983).
[9] Bascom, W. D. and Hunston, D. L., "The Fracture Behavior of Epoxy and Elastomer-Modified Epoxy Polymers," in *Rubber-Toughened Plastics*, ACS Adv. in Chem. Ser. 222, C. K. Riew, Ed. (ACS, Washington, DC, 1989), Chap. 6, pp. 135–172.
[10] Hunston, D. L., Rushford, J. L., Bitner, J. L., Oroshnik, J. and Rose, W. S., *J. Elast. Plast.* **12**, 133–149 (1980).
[11] Bitner, J. L., Rushford, J. L., Rose, W. S., Hunston, D. L. and Riew, C. K., *J. Adhesion* **13**, 3–28 (1981).
[12] Hunston, D. L. and Bullman, G. W., *Int. J. Adhesives & Adhesion* **5**, 69–74 (1985).
[13] Huang, Y. and Kinloch, A. J., *J. Adhesion* **41**, 5–22 (1993).
[14] Du, J., Thouless, M. D. and Yee, A. F., *Inter. J. Fracture* **92**(3), 271–285 (1998).
[15] Du, J., Niven, P. C., Thouless, M. D. and Yee, A. F., *Polym. Mat. Sci. Eng.* **79**, 103–105 (1998).
[16] Du, J., Thouless, D. D. and Yee, A. F., *Acta Materialia* **48**(13), 3581–3592 (2000).
[17] Thouless, M. D., Du, J. and Yee, A. F., "Mechanics of Toughened Brittle Polymers," in ACS Series: *Toughened Polymers*, Pearson, A., Yee, A. F. and Su, H. J., Eds., in press.
[18] Hoffman, D. K., Kolb, G. C., Arends, C. B. and Stevens, M. G., *Polym. Prep. Am. Chem. Soc., Div. Polym. Chem.* **26**(1), 232–233 (1985).
[19] Hoffman, D. K. and Arends, C. B., US Patent 4,708,996 (Nov. 24, 1987).
[20] Hoffman, D. K. and Kolb, G. C., *Polym. Mat. Sci. Eng.* **63**, 593–599 (1990).
[21] Hoffman, D. K., Oritz, C., Hunston, D. L. and McDonough, W. G., *Polym. Mat. Sci. Eng.* **70**, 7–8 (1994).
[22] Oritz, C., Hunston, D. L., McDonough, W. G. and Hoffman, D. K., *Polym. Mat. Sci. Eng.* **70**, 9–10 (1994).
[23] He, J., Ph. D. Thesis, *The Influence of Morphology and Concentration on Toughness in Dispersions Containing Preformed Acrylic Elastomer Particles in an Epoxy Matrix*, Howard University, Washington, DC, 1999.
[24] Raghavan, D., Hunston, D., He, J. and Hoffman, D., *Polym. Mat. Sci. Eng.* **79**, 194–195 (1998).
[25] He, J., Raghavan, D., Hunston, D. and Hoffman, D., *Polymer* **40**, 1923–1933 (1999).
[26] Hunston, D. L., He, J., Raghavan, D. and Hoffman, D. K., "Limits on Toughening of Epoxies," in *Proceedings of Adhesion Society Meeting* (Adhesion Society, Blacksburg, VA, 1998) p. 200.

[27] Hunston, D. L., He, J., Raghavan, D. and Hoffman, D., "Load History Dependence of Fracture in Rubber-Toughened Epoxies," in *Proceedings of Adhesion Society Meeting* (Adhesion Society, Blacksburg, VA, 2000) p. 10.
[28] Raghavan, D., Gu, X., Nguyen, T., VanLandingham, M. and Karim, A., *Macromolecules* **33**(6), 2573–2583 (2000).
[29] Raghavan, D., VanLandingham, M., Gu, X. and Nguyen, T., *Langmuir* **16**(24), 9448–9459 (2000).
[30] Raghavan, D., Gu, X., Nguyen, T. and VanLandingham, M., *J. Polym. Sci. Polym., Phys. Ed.*, **39**(13), 1460–1470 (2001).